CHEMISTRY
A EUROPEAN JOURNAL

DOI: 10.1002/chem.200600558

Metal–Salen-Base-Pair Complexes Inside DNA: Complexation Overrides Sequence Information

Guido H. Clever, Yvonne Söltl, Heather Burks, Werner Spahl, and Thomas Carell*[a]

Abstract: Two isomeric salicylic aldehyde nucleobases have been prepared and incorporated into various DNA duplexes. Reaction with ethylenediamine leads to formation of the well-known salen ligand inside the DNA double helix. Addition of transition-metal ions such as Cu^{2+}, Mn^{2+}, Ni^{2+}, Fe^{2+}, or VO^{2+} results in the formation of metal–salen-base-pair complexes, which were studied by using UV and circular dichroism (CD) spectroscopy. HPLC and ESI mass spectrometric measurements reveal an unusually high stability of the DNA–metal system. These metal–salen complexes act as interstrand cross-links and thereby lead to a strong stabilization of the DNA duplexes, as studied by thermal de- and renaturing experiments. Complex formation is strong enough to override sequence information even when the preorganization of the ligand precursors is unfavorable and the DNA duplex is distorted by the metal complexation. Furthermore, melting-point studies show that the salen complex derived from ligand **2** fits better into the DNA duplex, in accordance with results obtained from the crystal structure of the corresponding copper–salen complex **8**.

Keywords: circular dichroism · DNA structures · DNA · nucleobases · transition metals

Introduction

The molecular structure of DNA has fascinated scientists since the report of its elucidation by Watson and Crick in 1953.[1] The ascent of molecular genetics is directly based on this discovery and has led to revolutionary changes in the science of biology. Modern techniques of molecular biology, like cloning, the polymerase chain reaction (PCR), and DNA sequencing, would be unimaginable without knowledge of the structure of DNA and the mechanisms of semiconservative replication.

In contemporary chemistry, the synthesis of novel DNA-like structures is of tremendous interest. Recent examples include the synthesis of new base-pairing systems based on altered sugar components such as TNA,[2] pRNA, and homoDNA,[3] or the preparation of DNA-like materials with extended nucleobases.[4]

A more recent development is the design of metal–base-pairs in which the hydrogen bonds, which are typically used by nature to form the DNA duplex, are replaced by metal coordination interactions.[5] This concept may in the future allow a switching of the DNA single-strand interaction due to the presence or absence of specific metals. The motivation to incorporate metals into a DNA double helix in a defined fashion reaches far beyond the development of new base-pairing modes, however, as metal ions tightly coordinated inside the chiral double helix provide the possibility to generate new catalysts for enantioselective transformations. Here, the chiral environment established by the DNA is, in principle, amenable to optimization using evolutionary techniques.[6]

A second line of interest behind the incorporation of metal–base-pairs into DNA is the desire to program the construction of metal arrays. Solid-phase DNA synthesis allows the synthesis of highly modified DNA in which several metals may be stacked on top of each other. This provides new perspectives for the nanotechnological exploitation of the DNA structure as a molecular wire or as an electronic switch.[7] From an inorganic chemists' point of view, access to a variable set of multidentate ligands is of great interest to study metal interactions in homo- or heterometallic coordination compounds.

We recently reported a metal–salen-base-pair complex in DNA that accepts a variety of metal ions. This metal–base-pair complex yielded the highest ever reported duplex stabilization in terms of melting-point increase.[8] In contrast to

[a] Dipl.-Chem. G. H. Clever, Dipl.-Chem. Y. Söltl, H. Burks, Dr. W. Spahl, Prof. Dr. T. Carell
Department of Chemistry and Biochemistry
Ludwig Maximilians University Munich
Butenandtstrasse 5–13, Haus F, 81377 Munich (Germany)
Fax: (+49) 089-2180-77756
E-mail: Thomas.Carell@cup.uni-muenchen.de

all other known metal–base-pair complexes, the salen concept combines a covalent cross-link of both DNA single strands with the metal complexation event (Figure 1), and we showed that the assembly of the salen complex inside DNA proceeds cooperatively—the diamine is needed to form the ligand, while the coordinated metal prevents hydrolysis of the formed imines.

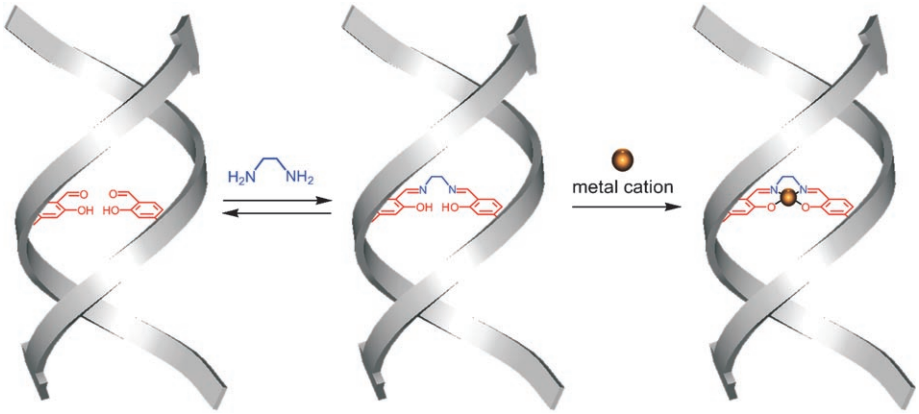

Figure 1. Assembly of the metal–salen-base-pair complex in the DNA double helix.[8]

Here we report a detailed investigation of the formed metal–base-pair complex in DNA, including thermal de- and renaturing studies, UV and circular dichroism (CD) spectroscopy measurements, and high-resolution mass spectrometry. The influence of the nucleoside geometry and variation of the sequence context on the complex formation and duplex stability are also examined. The precursors for the assembly of the metal–salen-base-pair complexes are the salicylic aldehyde nucleobases **1** and **2** (Figure 2). A comparison of oligonucleotides containing either ligand **1** or its isomer **2** by melting-point experiments shows that nucleoside **2** leads to a higher duplex stabilization upon complex formation. Furthermore, the superposition of the crystal structure of the copper–salen base pair **8** (derived from nucleoside **2**) with a natural AT Watson–Crick base pair shows a surprisingly large geometrical match. We present spectroscopic data supporting the assembly process of the metal–salen-base-pair complex inside the DNA duplex and we address the question of chirality transfer from the double helix to the metal complex. Finally, ESI-ICR (ICR = ion cyclotron resonance) mass spectrometry experiments provide detailed information about the integrity and stability of the metal–base-pair-containing DNA. We observe that the formation of the metal–salen cross-link overrides geometrical constraints preset by the nucleoside geometry or the DNA sequence context in all cases. Formation of the complex always occurs, even when the double helical structure is strongly distorted or when one native base pair has to be broken.

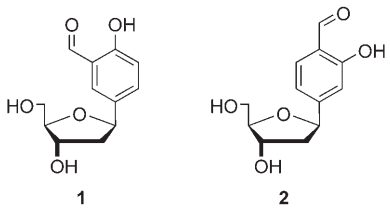

Figure 2. Salicylic aldehyde nucleosides **1** and **2** used to prepare the salen complexes in the DNA strands described in this study.

Results and Discussion

Synthesis of nucleoside 1 and its incorporation into desoxyoligonucleotides: The salicylic aldehyde nucleoside **1** was prepared according to the previously reported procedure for preparation of its isomer **2** (Scheme 1).[8]

This synthesis requires protection of both the carbonyl and hydroxyl groups of the salicylic aldehyde; this was performed bearing in mind that the protecting groups must be compatible with the organometallic *C*-glycosidation and subsequent solid-phase DNA synthesis. Furthermore, both protecting groups have to be cleaved under mild conditions after DNA synthesis to avoid degradation of the oligonucleotide. Commercially available 5-bromosalicylic aldehyde (**3**) was first protected as a 1,3-dioxane and was then treated with TIPS-Cl to yield the protected ligand **4**. Compound **4** was treated with two equivalents of *tert*-butyllithium to achieve a bromine–lithium exchange. The transmetalation of the organolithium compound to copper(I) is the most critical step in the *C*-glycosidation procedure. The reaction was found to work best when the lithiated ligand was transferred to a suspension of $CuBr{\cdot}SMe_2$ in freshly dried diethyl ether at −78 °C. Careful warming of this mixture to −30 °C until all solids had dissolved to give a clear yellow solution yielded the corresponding organocopper species, which turned out to be very unstable. It was therefore treated immediately with a solution of **5** in dry dichloromethane at −78 °C to give compound **6**. For the desired β-anomer, the configuration at C-1′ was assigned by evaluation of the nuclear Overhauser effect between the hydrogen atoms C1′-H, C2′-H, and C3′-H. The through-space coupling between C1′-H and α-C2′-H as well as between β-C2′-H and C3′-H lead to the appearance of cross-peaks in the NOESY NMR spectrum of nucleoside β-**6**. Attempts to increase the overall yield of the β-nucleoside by transforming a fully deprotected α-nucleoside into its β-anomer by acid treatment, as described for unsubstituted aryl-*C*-nucleosides,[9] resulted in decomposition of compound α-**6**. Deprotection of the sugar hydroxyl groups by transesterification in methanol[10] was followed by 5′-DMT protection and genera-

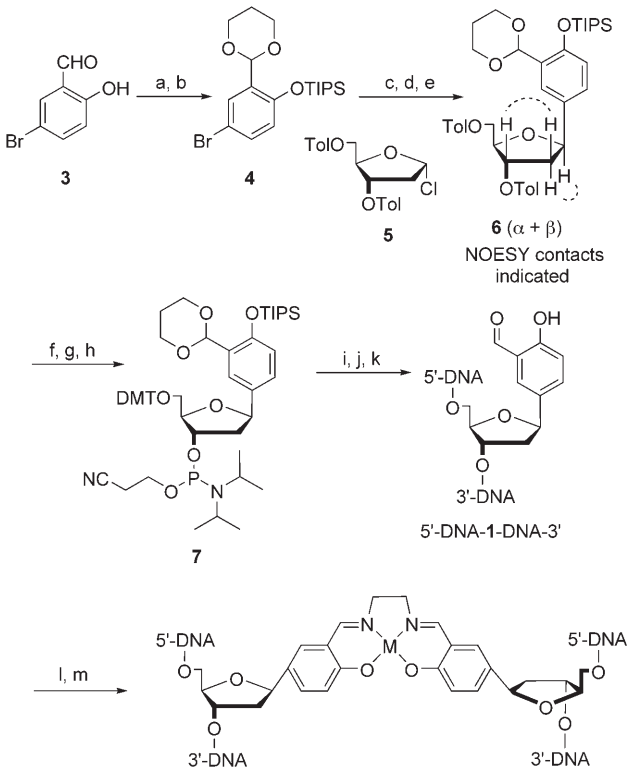

Scheme 1. Synthesis of phosphoramidite **7** and its incorporation into various DNA strands. a) 1,3-propanediol, $HC(OEt)_3$, $N(nBu)_4Br_3$, RT, 24 h, 96%; b) TIPS-OTf, $NEt(iPr)_2$, CH_2Cl_2, RT, 12 h, 95%; c) 2 equiv *t*BuLi, Et_2O, −78 °C, 2 h; d) CuBr·SMe_2, −78 °C to −30 °C, 20 min; e) **5**, CH_2Cl_2, 12 h, −78 °C to RT, 10% (only β-anomer isolated); f) K_2CO_3, CH_3OH, RT, 2 h, 43%; g) DMT-Cl, pyridine, 3 h, 55%; h) CED-Cl, $NEt(iPr)_2$, THF, RT, 2 h, 92%; i) automated DNA synthesis; j) deprotection of aldehydes with water-containing 2% $CHCl_2COOH$ in CH_2Cl_2; k) cleavage from solid support and cleavage of TIPS with $NH_{3(aq)}$/EtOH (3:1); l) hybridization of matching sequences under stringent conditions (Table 1); m) addition of excess ethylenediamine (en) and 1 equiv of metal ions (Table 1). CED-Cl = (2-cyanoethyl)-*N*,*N*-diisopropylchlorophosphoramidite, DMT = 4,4′-dimethoxytrityl, Tf = trifluoromethanesulfonyl, TIPS = triisopropylsilyl, Tol = toluyl.

tion of the phosphoramidite **7**. DNA synthesis was performed on an Äkta Oligopilot 10 synthesizer using a standard desoxyoligonucleotide protocol. The use of controlled-pore-size glass beads (CPG) as solid support material was found to give the desired oligonucleotides in excellent yields and with high purity. Treatment of the support-bound oligonucleotides with water containing 2% dichloroacetic acid in dichloromethane allowed removal of the acetal protecting groups without causing measurable depurination. The TIPS protecting groups were then removed smoothly and the DNA strands cleaved from the solid support by treatment with saturated aqueous ammonia/ethanol (3:1) at room temperature overnight. In the ammonia-containing solution, the unprotected aldehydes are in equilibrium with their corresponding yellow aldimines, which give broad and multiple peaks in the HPL chromatogram. It was subsequently found that addition of 20% acetic acid prior to the chromatographic separation process quantitatively cleaved the imines to the colorless aldehydes, which simplified the chromatographic purification. All oligonucleotides were finally desalted on C_{18} columns and the DNA was stored in water at −20 °C. A list of the prepared DNA strands used for this study can be found in Figure 4.

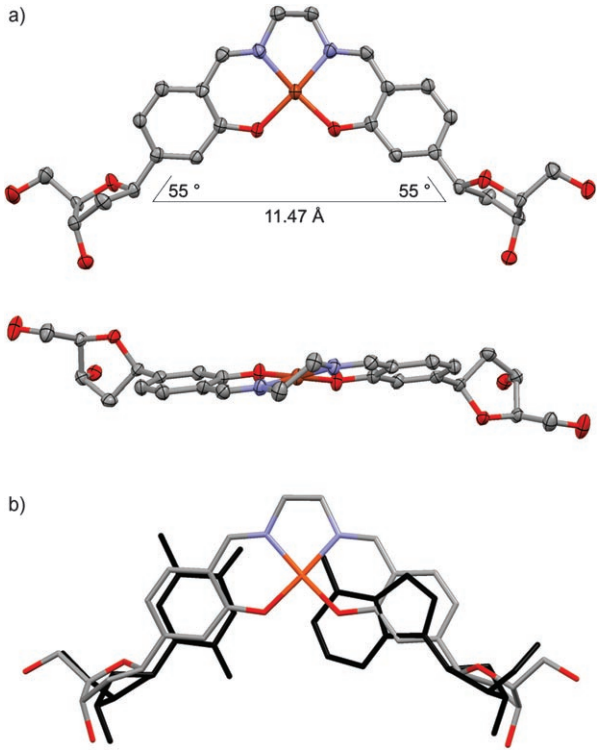

Figure 3. a) Top and side views of the crystal structure of compound **8**; b) Superposition of **8** (colored) with an AT base pair (black).

Crystal structure of the metal–salen-base-pair complex: Removal of all protecting groups from the β-nucleoside yielded compound **2**, which was subsequently treated with half an equivalent of ethylenediamine (en) in methanol to give the salen ligand. Treatment of the chelate ligand with one equivalent of $[Cu(acac)_2]$ in methanol yielded the copper–salen complex **8** as a purple solution, from which dichroic green-purple crystals were grown by slowly cooling this solution from 65 °C down to room temperature (Scheme 2).[11]

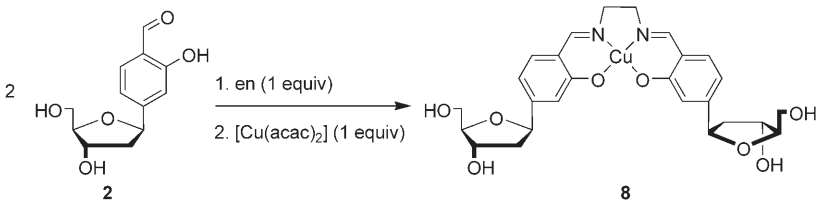

Scheme 2. Synthesis of the copper–salen complex **8**.

The crystal structure of complex **8** is depicted in Figure 3a. The metal–base-pair complex displays a tetrahedrally distorted square-planar coordination geometry of the copper center similar to that reported for related copper–

9-L^1-a: 5′-CACATTA**L^1**TGTTGTA-3′
9-L^1-b: 3′-GTGTAAT**L^1**ACAACAT-5′

9-L^2-a: 5′-CACATTA**L^2**TGTTGTA-3′
9-L^2-b: 3′-GTGTAAT**L^2**ACAACAT-5′

10-L^2-a: 5′-CACATT**L^{2}D**TGTTGTA-3′
10-L^2-b: 3′-GTGTAA**DL^2**ACAACAT-5′

11-L^2-a: 5′-CACATT**L^{2}DD**GTTGTA-3′
11-L^2-b: 3′-GTGTAA**DDL^2**CAACAT-5′

9-L^2-a: 5′-CACATT AL^{2}TGTTGTA-3′
12-L^2-b: 3′-GTGTAL^{2}T TACAACAT-5′

13-L^2-a: 5′-CACATT**DL^{2}D**GTTGTA-3′
13-L^2-b: 3′-GTGTAA**DL^{2}D**CAACAT-5′

14-L^2: 5′-GTAGAL^{2}TTTTL^{2}TCTAC-3′

15-L^2: 5′-GTAL^{2}AGTTTTCTL^{2}TAC-3′

Figure 4. Sequences of the examined oligonucleotides. $\mathbf{L^1}=\mathbf{1}$ and $\mathbf{L^2}=\mathbf{2}$. **D** = tetrahydrofuran spacer (1′,2′-desoxyribose).

salen complexes.[12] The chelate rings exhibit a Δ configuration that resembles surprisingly closely the propeller twist of a native Watson–Crick base pair. The dihedral angle, θ_P, between the planes defined by the aromatic rings was found to be +22°. This is slightly larger than in natural base pairs (ca. +10°) but of the same sign. The salicylic aldimine moieties are oriented in an *anti* conformation with respect to the sugars, and the distance between the C1′ atoms of the two sugars is 11.47 Å, which is close to the values of 10.44 and 10.72 Å for AT and GC Watson–Crick base pairs, respectively. The angle between the *C*-glycosidic bond and the line connecting the C1′ atoms (55°) is in excellent agreement with that of a normal base pair. The 2′-desoxyribose sugar rings exhibit a C2′-*endo* ("south") conformation, which is common for B-type DNA.[13] The molecule has a C_2 axis that passes through the copper atom and the middle of the ethylene bridge. The superposition depicted in Figure 3b shows the high geometrical match of the desoxyribosyl-substituted Cu–salen complex and a normal AT Watson–Crick base pair. No circular dichroism was observed for a solution of **8** in water.

Thermal de- and renaturation studies: To determine the thermal stability of DNA duplexes containing the ligand precursors **1** and **2**, melting-point measurements in the absence and presence of diamines and metal ions were performed. The results are summarized in Table 1.

From the melting-point data it is evident that all oligonucleotides containing ligand **1** are less stable than those with nucleoside **2**. The base analogue **2** seems to orient the salicylic aldehydes inside the DNA duplex in a way that offers perfect preorganization for the desired complex formation. The melting point of duplex **9-L^2-a/b** (containing ligand **2**) is increased by about 5 K upon addition of only ethylenediamine. A similar effect is observed for duplex **9-L^1-a/b** (Table 1, entries 1, 2, 5, and 6). This stabilizing effect due to

Table 1. Melting-point experiments with the oligonucleotides **9**–**14**.

Entry	Strand(s)[a]	Additive(s)		T_M [°C]
1	**9-L^1-a/b**		[b]	35.7
2	**9-L^1-a/b**	100 μM en	[b]	40.5
3	**9-L^1-a/b**		4 μM Cu^{2+}[b]	36.8
4	**9-L^1-a/b**	100 μM en	4 μM Cu^{2+}[b]	71.6
5	**9-L^2-a/b**		[b]	39.9
6	**9-L^2-a/b**	100 μM en	[b]	45.0
7	**9-L^2-a/b**		4 μM Cu^{2+}[b]	54.9
8	**9-L^2-a/b**	100 μM en	4 μM Cu^{2+}[b]	82.4
9	**9-L^2-a/b**		[c]	40.7
10	**9-L^2-a/b**	100 μM en	4 μM Mn^{2+}[c]	68.8[d]
11	**10-L^2-a/b**		[b]	32.0
12	**10-L^2-a/b**	100 μM en	4 μM Cu^{2+}[b]	66.8[e]
13	**10-L^2-a/b**		[c]	33.4
14	**10-L^2-a/b**	100 μM en	6 μM Mn^{2+}[c]	60.6[d]
15	**11-L^2-a/b**		[b]	18.6
16	**11-L^2-a/b**	100 μM en	4 μM Cu^{2+}[b]	59.1
17	**11-L^2-a/b**		[c]	20.6
18	**11-L^2-a/b**	100 μM en	4 μM Mn^{2+}[c]	53.2[d]
19	**13-L^2-a/b**		[b]	20.9
20	**13-L^2-a/b**	100 μM en	4 μM Cu^{2+}[b]	56.5[e]
21	**13-L^2-a/b**		[c]	21.0
22	**13-L^2-a/b**	100 μM en	6 μM Mn^{2+}[c]	57.8[d]
23	**14-L^2**		[b]	35.4
24	**14-L^2**	100 μM en	[b]	52.2
25	**14-L^2**	100 μM en	4 μM Cu^{2+}[b]	76.5
26	**14-L^2**		[c]	36.0
27	**14-L^2**	100 μM en	[c]	51.6
28	**14-L^2**	100 μM en	4 μM Mn^{2+}[c]	70.3[d]
29	**9-L^2-a/b**	100 μM edh	[b]	73.4[f]

[a] For sequences, see Figure 4. All samples contained 3 μM DNA (duplex or hairpin) and 150 mM NaCl. Melting profiles were measured from 0 to 85 °C (95 °C for Cu^{2+}) with a slope of 0.5 °C min^{-1}. [b] All experiments using Cu^{2+} and corresponding controls were carried out in 10 mM Ches (*N*-cyclohexyl-2-aminoethanesulfonic acid) buffer at pH 9.0. [c] All experiments using Mn^{2+} and corresponding controls were carried out in 10 mM Hepes (*N*-(2-hydroxyethyl)piperazine-*N*′-(2-ethanesulfonic acid)) buffer at pH 9.0. [d] Reproducible differences in de- and renaturing profiles due to thermal instability of the Mn complex. The given melting points correspond to the denaturing profiles. [e] Additional transition of low intensity (entry 12: 23.8 °C; entry 20: 16.0 °C). [f] edh = *O*,*O*′-ethylenedihydroxyamine. Entries 5–10 are reproduced from reference .[8]

the cross-linking of both strands by ethylenediamine is, however, surprisingly small. The reason for this is that formation of the imine linkage in water is highly reversible, which causes rapid hydrolysis of the cross-link during the melting-point experiment.[14] The better geometrical fit of the salen complex based on nucleobase **2** is particularly obvious after addition of only Cu^{2+} ions (no ethylenediamine). Only the perfectly preoriented system **9-L^2-a/b** accepts the metal, which results in a strong stabilization. Duplex **9-L^1-a/b**, in contrast, shows no stabilizing effect upon addition of Cu^{2+} ions, thus indicating that in a duplex where two salicylic aldehydes **1** face each other as a base pair, metal coordination between them is impossible (Table 1, entries 3 and 7). However, addition of ethylenediamine and copper results in dramatic melting-point increases for both duplexes (Table 1, entries 4 and 8), thus showing the strong cooperativity of the complex formation in DNA. The complexed metal prevents hydrolysis of the imine bonds. The stability of the rigid salen complex is seemingly so dominating that its formation

occurs even when the preorganization of the salicylic aldehyde precursors in DNA is not optimal (as in duplex **9-L^1-a/b**). The energetic gain upon forming the complex is so large that the system can tolerate the distortion of the DNA double helix. In this situation, complex formation in DNA occurs first and hence controls the final duplex geometry.

The degree of stabilization is again higher for duplex [**9-L^2-a/b**+en+Cu], which is another indication that the salen ligand based on salicylic aldehyde **2** fits better into the duplex. The discussed melting points are compared in Figure 5.

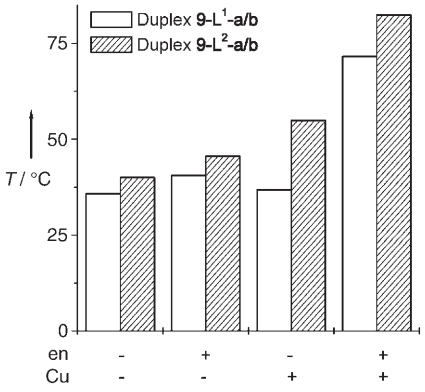

Figure 5. Comparison of the thermal stability of duplexes **9-L^1-a/b** and **9-L^2-a/b** upon addition of ethylenediamine and/or Cu^{2+}.

In order to investigate how the preorganization of the salicylic aldehydes in the duplex effects metal–salen complex formation in more detail, we systematically varied the position of the two salicylic aldehydes in the oligonucleotide sequence, as depicted in Figure 6. In these constructs, we chose a simple tetrahydrofuran-derived spacer (**D** in Figure 4), which does not lead to any unwanted interaction with the ligands, as counterbase to the aldehydes. A graphical comparison of the determined thermal stabilities of the original strand **9-L^2-a/b** with the sequences **10-L^2-a/b** and **11-L^2-a/b** is displayed in Figure 6 (the sequences are depicted in Figure 4). The melting points of the bare duplexes decrease by about 8 K upon loss of the first and by another 14 K upon loss of a second AT base pair. The values for the strands after assembly of the metal–salen-base-pair complex follow the same trend (Table 1, entries 11–14 and 15–18). However, duplexes **10-L^2-a/b** and **11-L^2-a/b**, in which the aldehydes are shifted by one or two positions, respectively, are still able to form interstrand salen complexes with ethylenediamine

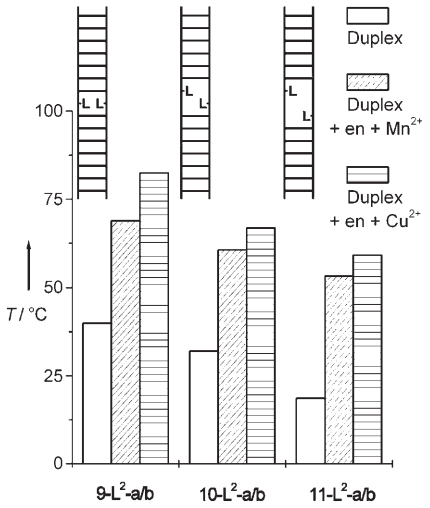

Figure 6. Comparison of the thermal stabilities of duplexes **9-L^2-a/b**, **10-L^2-a/b**, and **11-L^2-a/b** without any additives, with en and Mn^{2+}, and with en and Cu^{2+}.

and manganese or copper as the metal. Complex formation even works when the salicylic aldehydes are shifted as in **11-L^2-a/b** but separated by an AT base pair, as in the duplex **9-L^2-a/12-L^2-b**. The addition of ethylenediamine and Cu^{2+} to this duplex leads to a complex melting behavior that differs significantly from the melting curve of the pure duplex (not shown). Furthermore, mass spectrometric analysis shows the quantitative formation of the duplex containing one copper–salen complex (Table 2, entry 11). Consequently, the formation of the salen complex in the duplex [**9-L^2-a/12-L^2-b**+en+Cu] must have broken the AT base pair between the two salicylic aldehydes. The formation of the salen complex is obviously so strong that it forces the DNA duplexes to accept unfavorable double helical structures and even one broken base pair. That the double helix plays a role in complex formation became obvious when we analyzed the single-strand composition of the duplex as we were unable to detect any homoduplexes (a/a or b/b) by mass spectro-

Table 2. ESI mass spectrometry experiments with the oligonucleotides **9**, **13**, and **15**.

Entry	Strand(s)[a]	Additive(s)		Species	Calcd mass	Exptl mass	Δ [ppm]
1	**15-L^2**			$[M-4H]^{4-}$	1209.4573	1209.4497	6.3
2	**15-L^2**	en	Mn^{3+}	$[M-5H]^{4-}$	1228.4364	1228.4376	1.0
3	**15-L^2**	en	Cu^{2+}	$[M-4H]^{4-}$	1230.6999	1230.6908	7.4
4	**15-L^2**	en	Fe^{3+}	$[M-5H]^{4-}$	1228.6967	1228.6902	5.3
5	**15-L^2**	en	VO^{2+}	$[M-4H]^{4-}$	1231.6997	1231.6973	1.9
6	**15-L^2**	en	Ni^{2+}	$[M-4H]^{4-}$	1229.4488	1229.4299[b]	15.4
7	**9-L^2-a/b**			$[M_a-4H]^{4-}$	1136.6993	1136.6887	9.3
				$[M_b-4H]^{4-}$	1141.2048	1141.1948[c]	8.8
8	**9-L^2-a/b**	en	Cu^{2+}	$[M-9H]^{9-}$	1021.7207	1021.7220	1.3
9	**13-L^2-a/b**	edh[d]		$[M-9H]^{9-}$	961.3902	961.3792	11.4
10	**15-L^2**	phen[d]	Cu^{2+}	$[M-9H]^{9-}$	1242.6998	1242.6840	12.7
11	**9-L^2-a/12-L^2-b**	en	Cu^{2+}	$[M-9H]^{9-}$	1020.7297	1020.7259	3.7

[a] For sequences see Figure 4. All samples contained 30 μM DNA (duplex or hairpin) and 100 mM NH_4OAc (pH 8). DNA strands were first hybridized by slow cooling from 80 to 25 °C and then incubated for at least 12 h with the diamine and a solution of the metal sulfate at room temperature. [b] Additional peaks for [**15-L^2**+en+2Ni−2H_2O−4H^+] and [**15-L^2**+en+3Ni−2H_2O−6H^+] were observed. [c] Only single-strand masses observed. [d] edh = *O*,*O*′-ethylenedihydroxyamine, phen = 1,2-phenylenediamine.

metric analysis—the metal was always complexed inside the correct heteroduplexes (a/b). These results indicate that the two single strands have to form a stable duplex and that this seems to be a prerequisite for complex formation. In the duplex, however, complex formation takes place even if the double helix is distorted afterwards. Formation of [**9-L^2-a/12-L^2-b**+en+Cu] demonstrates that the complex formation is even able to override sequence information.

The double helix **13-L^2-a/b**, in which the facing salicylic aldehydes are flanked by the spacers **D** on either side, shows a similar behavior in the melting-point experiments (Table 1, entries 19–22).

Hairpin **14-L^2** carries the metal–base-pair complex right next to a TTTT loop such that the metal complex closes the hairpin and presents the metal to the core of a chiral cavity. In this case formation of metal–salen complexes with either Mn^{2+} or Cu^{2+} can also be observed in the thermal de- and renaturing curves.

Finally, we also varied the diamine bridge. Because imine formation in the absence of a coordinated metal is reversible, we used hydroxylamine derivatives as they give much more stable oximes. These oximes indeed result in cross-linking, even in the absence of any coordinating metal ions. For example, addition of *O*,*O*′-ethylenedihydroxyamine to duplex **9-L^2-a/b** caused bridging of the two strands and an increase of T_M by 33.5 K (Table 1, entry 29). In addition, the molecular ion of the duplex was observed in the ESI mass spectrum (see below). 1,2-Phenylenediamine can also be used as the cross-linking bridge, provided oxygen is excluded (Table 2, entry 10).

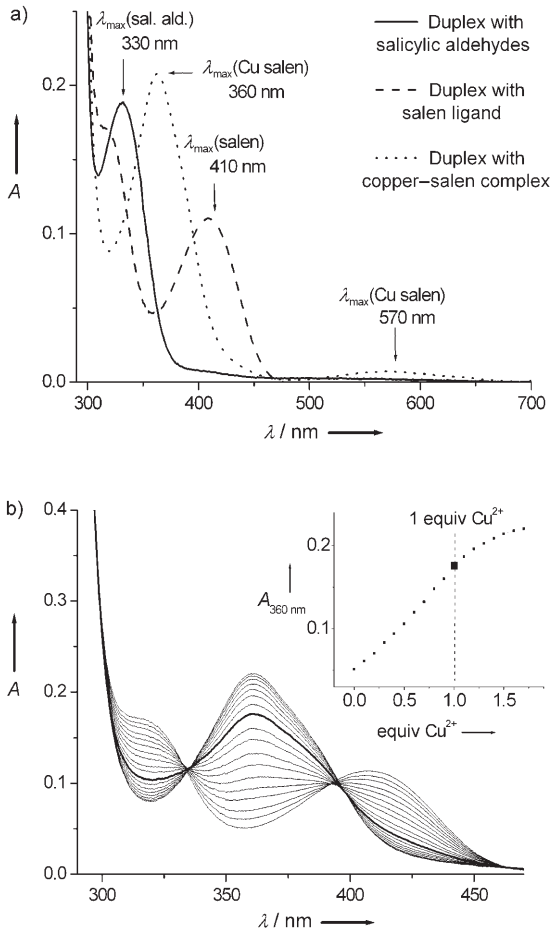

Figure 7. a) Electronic absorption bands of duplexes **9-L^2-a/b**, [**9-L2-a/b**+en], and [**9-L^2-a/b**+en+Cu]; b) Titration of [**9-L2-a/b**+en] (30 μM DNA, 1 mM en, 100 mM $NH_4OAc_{(aq)}$, pH 8) with Cu^{2+} in steps of 0.1 equiv; thick line: 1.0 equiv Cu^{2+}; inset: plot of Abs_{360} against the ratio [Cu^{2+}]/[**9-L2-a/b**+en].

UV/Vis and CD spectroscopy: Further insight into the formation of the interstrand salen ligand and the complexation of divalent metal ions was obtained by monitoring of the assembly process by means of UV/Vis spectroscopy. The duplex **9-L^2-a/b** has an absorption maximum at $\lambda = 260$ nm, as expected for a double strand consisting primarily of natural nucleobases.[13] The salicylic aldehydes give rise to an additional absorption at $\lambda = 330$ nm due to the $\pi \rightarrow \pi^*$ transition of the aromatic chromophore.[15] Addition of an excess of ethylenediamine resulted in the appearance of a new band at $\lambda = 410$ nm. At the same time, the absorption of the salicylic aldehyde at $\lambda = 330$ nm decreased over 20 min. The absorption at $\lambda = 410$ nm matches the reported values for a deprotonated salen ligand. The existence of isosbestic points at $\lambda = 325$ and 358 nm indicates an immediate formation of the salen ligand when an ethylenediamine molecule encounters the preorganized salicylic aldehydes (not shown). In this model, the formation of the first imine bond is rate-determining and the second imine bond formation is accelerated for entropic reasons.

Coordination of Cu^{2+} ions by the preformed salen ligand in DNA results in a shift of the absorption band to $\lambda =$ 360 nm. In addition, a new band appears at $\lambda = 570$ nm, which is typical for the N_2O_2–Cu chromophore.[16] A titration of Cu^{2+} ions against the DNA duplex [**9-L2-a/b**+en] is shown in Figure 7b. The overlaid curves show isosbestic points at $\lambda = 334$ and 395 nm. The plot of the absorption at $\lambda = 360$ nm against the copper concentration shows a linear increase up to a duplex to Cu^{2+} ratio of about 1:1. The UV spectra of **9-L^2-a/b**, [**9-L2-a/b**+en], and [**9-L^2-a/b**+en+Cu] are shown in Figure 7a.

In contrast to our observation that an aqueous solution of the homochiral Cu–salen complex **8** shows no CD signal in the range between $\lambda = 300$ and 700 nm, the duplex [**9-L^2-a/b**+en+Cu] features a strong CD signal in the range of the absorption of the $\pi \rightarrow \pi^*$ transition (Figure 8). The observed signal has a positive sign in the high-energy region and a negative sign for the low-energy part and corresponds, according to studies by Downing et al., to a Δ configuration of the metal chelate inside the duplex.[16]

The salen complex adopts the same absolute configuration inside the DNA duplex as in the crystal (Figure 3). Concerning the metal-based d–d transition at around $\lambda =$ 570 nm, only a small CD effect is observed (Figure 8).

HPLC analysis of the copper–salen-containing duplexes: The unusually high stability of the copper–salen complex in

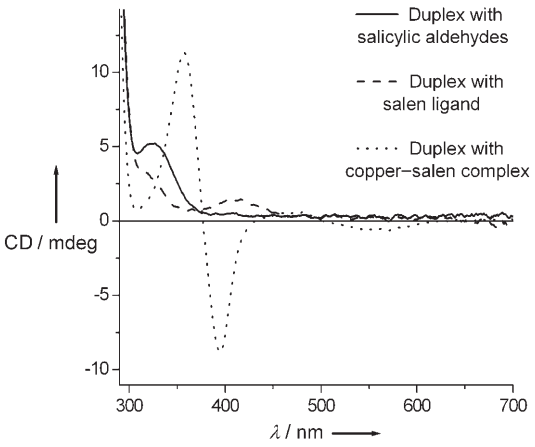

Figure 8. Circular dichroism spectra of **9-L²-a/b**, [**9-L2-a/b**+en], and [**9-L²-a/b**+en+Cu] (30 μM DNA, 1 mM en, 30 μM $CuSO_4$, 100 mM NH_4OAc, pH 8).

the DNA duplex has a great influence on the chromatographic behavior of the double strand **9-L²-a/b** (Figure 9).

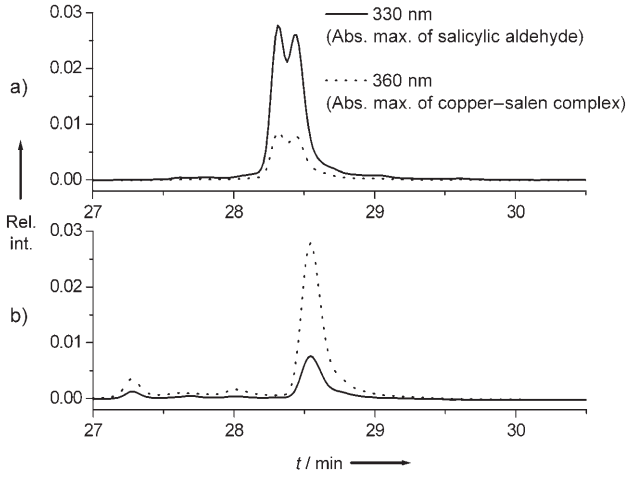

Figure 9. Comparison of HPL chromatograms of a) 30 μM **9-L²-a/b** in 100 mM NH_4OAc (pH 8) and b) the same sample after incubation with 1 mM ethylenediamine and 100 μM Cu^{2+}. Eluent: 2 mM $NHEt_3OAc$ in H_2O/CH_3CN; gradient: 0–40 % CH_3CN in 40 min.

Injection of a hybridized probe containing **9-L²-a/b** in NH_4OAc buffer (100 mM) onto a C_{18}-RP column resulted in complete denaturation of the duplex. Consequently, two peaks, one for each single strand, were observed. When we incubated the duplex sample with an excess of ethylenediamine and Cu^{2+} prior to injection, only one peak was observed. Analysis of this peak by using UV spectroscopy during the HPLC run revealed a bathochromic shift of the $\pi\rightarrow\pi^*$ band, which is indicative of the presence of the copper–salen complex. LC–MS analysis of the peak confirmed the exclusive presence of the Cu–salen duplex. This result shows that the Cu–salen-containing DNA duplexes are so stable that they can be isolated and purified by HPLC.

ESI-ICR mass spectrometry: We used a Thermo Finnigan LTQ-FT ESI-ICR mass spectrometer for the mass spectrometric characterization of the metal-containing duplexes.[17] The metal–DNA samples were prepared by hybridizing equimolar amounts of both single strands in ammonium acetate buffer (pH 8, 100 mM) and subsequent incubation with the diamine and the corresponding metal salt overnight at room temperature. In all cases, the experimentally found masses are in excellent agreement with the values calculated for the hairpins or duplexes containing one molecule of diamine and one metal ion. Table 2 shows the calculated molecular weights of the lowest-weight isotopomers along with the measured values (for m/z with $z=-4$ or -9). In each case, one molecule of diamine condenses with both salicylic aldehydes of the DNA strands, with the loss of two water molecules, to form the cross-linking ligand that binds the metal ion.

All the molecular weights obtained prove the presence of only one metal ion in the duplexes or hairpins (Table 2, entries 2–5). Interestingly, only in the case of Ni^{2+} were molecular weights obtained that indicate the presence of [**15-L²**+en+$2Ni^{2+}-2H_2O-4H^+$] and of [**15-L²**+en+$3Ni^{2+}-2H_2O-6H^+$] as well as the formation of the expected mono-Ni^{2+} adduct [**15-L²**+en+$Ni^{2+}-2H_2O-2H^+$]. These are a sign of further unspecific, but rather tight, binding of additional Ni^{2+} to the oligonucleotide once the salen ligand is saturated with metal.

Addition of Mn^{2+} and Fe^{2+} to the ligand-containing duplexes and hairpins resulted in oxidation to give Mn^{3+} and Fe^{3+} ions, as clearly proven by the m/z values.[18] The charge of the coordinated metal can be deduced from the observed m/z value by comparison with the simulated isotope pattern. Only the peaks expected for the coordination of one iron(III) ion to the assembled salen ligand, along with Na^+ and K^+ adducts, appear in the spectrum of [**15-L²**+en+$Fe^{3+}-2H_2O-3H^+$] (Figure 10a).

The mass spectrum of the duplex [**9-L²-a/b**+en+$Cu^{2+}-2H_2O-2H^+$] is shown in Figure 10b as an example. Only the peaks calculated for the Cu–salen-containing duplex are observed, along with some Na^+, K^+, and $NHEt_3^+$ adducts of it. No uncomplexed single strands are visible, and not more than one copper atom is complexed to the duplex.

The reaction of oligonucleotide duplex **13-L²-a/b** with *O*,*O*′-ethylenedihydroxyamine (edh) in the absence of metal ions results in quantitative cross-linking to give the bis-oxime compound [**13-L²-a/b**+edh$-2H_2O$] (Figure 10c).

Conclusion

We have synthesized DNA duplexes containing a new metal–base-pair complex derived structurally from the well-known salen ligand. The metal–salen-base-pair complex is assembled in oligonucleotide duplexes containing two salicylic aldehyde bases by addition of a diamine such as ethylenediamine and various transition-metal ions such as Cu^{2+}, Mn^{2+}, Ni^{2+}, Fe^{2+}, or VO^{2+}. Assembly of the salen com-

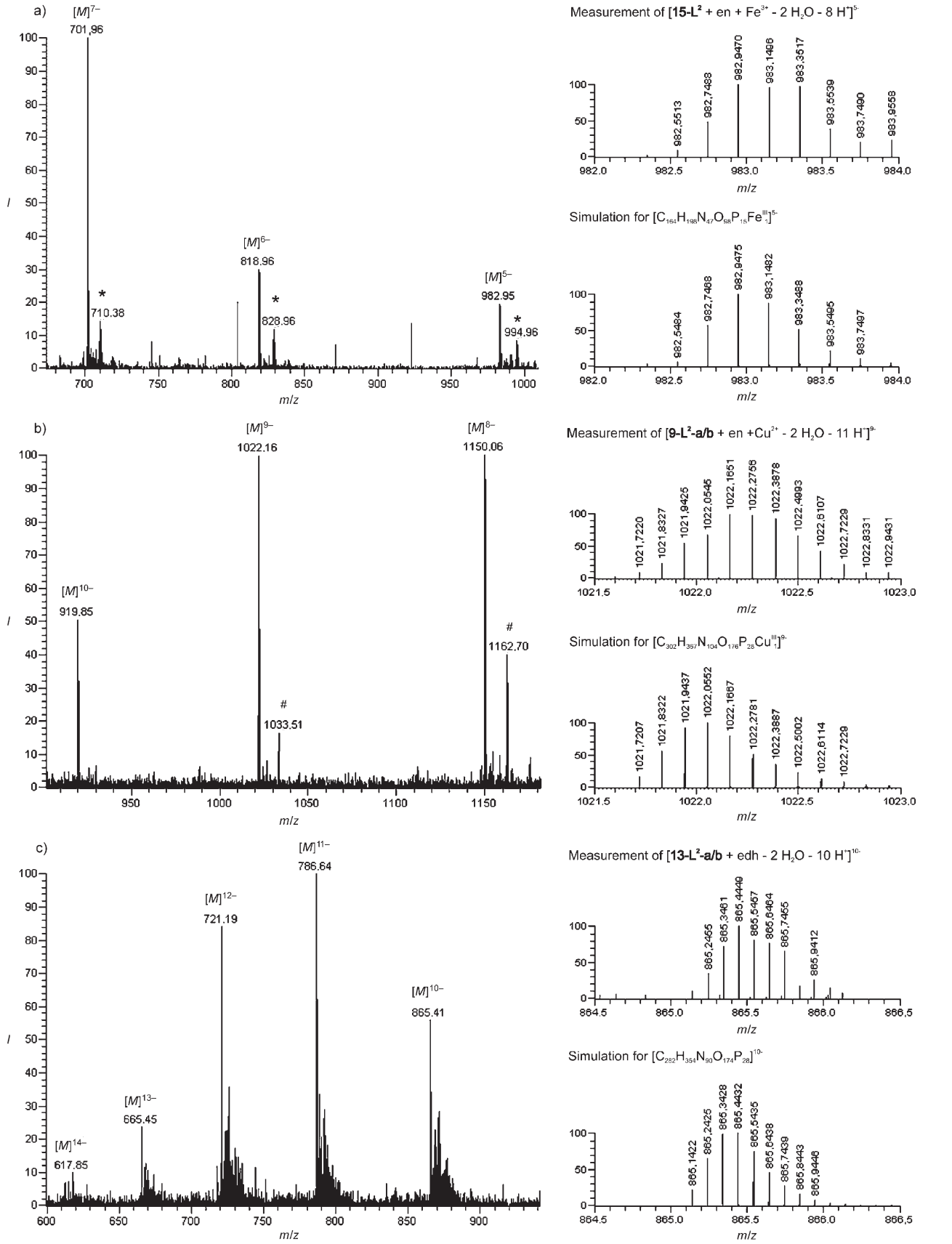

Figure 10. Selected ESI mass spectra and comparison of experimental data with calculated molecular weights. a) [**15-L²**+en+Fe^{3+}−$2H_2O$−$3H^+$]; b) [**9-L²-a/b**+en+Cu^{2+}−$2H_2O$−$2H^+$]; c) [**13-L²-a/b**+edh−$2H_2O$]; Adducts: *=[*M*+Na+K−2H], #=[*M*+NEt_3].

plexes resulted in tremendous stabilization of the duplex, as shown by HPLC and melting-point experiments. Two different isomers of salicylic aldehyde nucleobases were examined and it was found that the copper–salen complex derived from nucleoside **2** resulted in the highest duplex stabilization. A base pair formed by two of these ligands is able to complex metals even in the absence of the corresponding diamine. In accordance with these results, we found that the X-ray structure of **8** shows a very good geometrical fit with natural Watson–Crick base pairs. UV measurements confirm the reaction of two salicylic aldehyde nucleobases that face each other in the duplex with ethylenediamine to give the salen ligand, and addition of metal ions allows assembly of the metal complex inside the duplex. The CD spectra of the monomeric complex **8** and the interstrand complex show that the salen complex exists in the DNA as a Δ chelate. The sequence context of the oligonucleotide strands was also changed to test how the preorganization geometries affect metal complex formation. To our surprise, we observed that the salen complex formation has such a strong driving force that complex formation occurs even when the salicylic aldehydes are not directly facing each other in the duplex. High-resolution ESI-ICR mass spectra confirm the formation of discrete species consisting of the DNA double helix, one molecule of diamine, and one metal ion. The experimentally determined molecular weights match the calculated values to within a few parts per million. The reported findings bring us another step closer to being able to exploit the metal–salen-base-pair complex in bio-inspired nanotechnology.

Experimental Section

General: Chemicals were purchased from Sigma–Aldrich, ACROS, or Lancaster and were used without further purification. The solvents used were of reagent grade and were purified by using standard methods. The reactions were monitored on Merck Silica 60 F_{254} TLC plates. Detection was done by irradiation with UV light (254 nm) and staining with an acidic 2,4-dinitrophenylhydrazine solution in ethanol. Flash chromatography was performed on Silica 60 (Merck, 230–400 mesh). NMR spectra were recorded on Varian Oxford 200, Bruker AC 300, Varian XL 400, and Bruker AMX 600 spectrometers. Mass spectra were recorded on Finnigan MAT 95 (EI), Bruker Autoflex II (MALDI-TOF), and Thermo Finnigan LTQ-FT (ESI-ICR) spectrometers. IR spectra were measured on a Nicolet 510 FTIR spectrometer in a KBr matrix or with a diamond-ATR (Attenuated Total Reflection) setup. DNA synthesis was performed on a PerSeptive Biosystems Expedite 8900 Synthesizer and an Äkta Oligopilot 10 (Amersham Biosciences). Analytics and purification of the oligonucleotides were performed on Merck LaChrome HPLC systems with UV and diode-array detectors using 5-μ Silica-C_{18} RP columns and 0.1 M $NHEt_3OAc$ in H_2O/CH_3CN as eluent. UV spectra and melting profiles were measured on a Cary 100 UV/Vis spectrometer and CD spectra were measured on a JASCO J 810 CD-spectropolarimeter according to previously reported protocols.[8] The ESI spectra of DNA strands were measured in flow injection analysis mode or coupled to chromatographic separation (eluent: 2 mM $NHEt_3OAc$ in H_2O/CH_3CN). In flow injection mode, a 2-μL sample (30 μM DNA, 100 mM NH_4OAc) was injected in a steady flow of H_2O/CH_3CN (8:2; 200 μL min^{-1}). The capillary temperature was 300 °C, with a spray voltage of 4–5 kV (negative mode).

2-(5-Bromo-2-hydroxyphenyl)-1,3-dioxane (3a): 5-Bromosalicylic aldehyde (**3**; 6.0 g, 30 mmol) was mixed with triethyl orthoformate (5.20 mL, 31.2 mmol) and 1,3-propanediol (8.60 mL, 120 mmol). A catalytic amount of tetra-*n*-butylammonium tribromide (1.5 g, 3.1 mmol) was added and the mixture was stirred for 24 h at room temperature. The reaction was ended by adding saturated, aqueous $NaHCO_3$ until pH 7 was reached. The mixture was extracted twice with ethyl acetate (50 mL) and the combined organic extracts were washed with dilute, aqueous $NaHCO_3$ and dried with Na_2SO_4. The solvents were removed in vacuo and the raw material purified by using column chromatography (silica gel; hexane/EtOAc = 10:1) to give a colorless oil (7.46 g, 28.9 mmol, 96 %). ^{1}H NMR (400 MHz, $CDCl_3$): δ = 1.51 (d, J = 13.8, 1H), 2.19–2.31 (m, 1H), 4.00 (ddd, J = 12.3, 12.3, 2.6 Hz, 2H), 4.30 (ddd, J = 12.0, 5.0, 1.4 Hz, 2H), 5.60 (s, 1H), 6.78 (d, J = 9.3 Hz, 1H), 7.28–7.34 (m, 1H), 7.86 ppm (s, 1H); ^{13}C NMR (100 MHz, $CDCl_3$): δ = 25.6, 67.5, 101.9, 111.2, 119.1, 124.0, 130.4, 133.1, 154.1 ppm; IR (film): $\tilde{\nu}$ = 2972 (m), 2927 (w), 2863 (m), 2727 (w), 1724 (w), 1651 (w), 1618 (w), 1583 (w), 1485 (s), 1428 (m), 1390 (s), 1353 (m), 1277 (m), 1255 (s), 1237 (s), 1175 (m), 1151 (s), 1120 (s), 1095 (s), 1048 (w), 990 cm^{-1} (s); EI-HRMS: m/z calcd for $C_{10}H_{11}BrO_3$ $[M]^+$: 257.9892; found: 257.9900.

2-(5-Bromo-2-(triisopropylsilyloxy)phenyl)-1,3-dioxane (4): Compound **3a** (6.7 g, 26 mmol) was dissolved in dry dichloromethane (50 mL) and $NEt(iPr)_2$ (11.2 mL, 65.0 mmol) was added. Triisopropylsilyl triflate (8.4 g, 22 mmol) was then added dropwise at 0 °C. After stirring for 12 h at room temperature, water was added and the mixture was extracted twice with dichloromethane (50 mL). The combined organic extracts were washed with water and saturated, aqueous NaCl and dried with Na_2SO_4 . After removal of the solvents in vacuo, the resulting oil was subjected to column chromatography (first pure hexane to elute excess silyl reagent, then hexane/EtOAc (9:1)). The resulting colorless oil (10.3 g, 24.8 mmol, 95 %) was intensively dried under high vacuum before it was used for the next step. ^{1}H NMR (400 MHz, $CDCl_3$): δ = 1.11 (d, J = 7.3 Hz, 18H), 1.30 (sept, J = 7.3 Hz, 3H), 1.42 (d, J = 13.5 Hz, 1H), 2.16–2.28 (m, 1H), 3.94 (ddd, J = 12.3, 12.3, 2.5 Hz, 2H), 4.23 (dd, J = 10.7, 5.0 Hz, 2H), 5.81 (s, 1H), 6.66 (d, J = 8.7 Hz, 1H), 7.26 (dd, J = 8.7, 2.7 Hz, 1H), 7.71 ppm (d, J = 2.7 Hz, 1H); ^{13}C NMR (100 MHz, $CDCl_3$): δ = 13.0, 18.0, 25.8, 67.5, 96.7, 113.2, 119.9, 130.5, 130.9, 132.3, 152.3 ppm; IR (KBr): $\tilde{\nu}$ = 2946 (s), 2892 (m), 2867 (s), 2724 (w), 1730 (w), 1597 (w), 1578 (w), 1486 (s), 1468 (s), 1428 (w) 1409 (m), 1391 (s), 1277 (s), 1238 (m), 1181 (m), 1151 (m), 1127 (m), 1102 (s), 1006 (s), 957 (w), 917 (s), 881 cm^{-1} (s); ESI-HRMS: m/z calcd. for $C_{19}H_{32}BrO_3Si$ $[M+H]^+$: 417.1304; found: 417.1279.

Protected nucleoside 6: A solution of compound **4** (5.23 g, 12.6 mmol) in freshly distilled diethyl ether (20 mL) was cooled to −78 °C and *t*BuLi (16.9 mL, 26.5 mmol) in pentane (1.7 M) was added dropwise over one hour. The reaction was kept at −78 °C, with stirring, for 3 h and subsequently transferred with a cannula to a precooled (−78 °C) suspension of copper(I) bromide/dimethyl sulfide complex (1.3 g, 6.3 mmol) in diethyl ether (10 mL). The reaction mixture was carefully warmed to −30 °C for 20 min, whereupon the solids dissolved to give a yellow solution, which was immediately cooled to −78 °C and transferred with a cannula to a precooled solution of α-3′,5′-bistoluyl-1′-ribosyl chloride (**5**)[19] (1.64 g, 4.20 mmol) in dry dichloromethane (20 mL). The reaction mixture was allowed to warm up to room temperature overnight, then saturated NH_4Cl solution (20 mL), 2 M ammonia (1 mL), and diethyl ether (100 mL) were added and the organic phases were separated. The aqueous phases were extracted twice with diethyl ether (100 mL) and the organic phases combined. After washing twice with water, once with saturated NaCl solution, and drying over Na_2SO_4, the solvents were removed in vacuo and the resulting oil was purified by using flash column chromatography (silica gel; hexane/EtOAc = 10:1) to give the desired β-anomer (303 mg, 0.44 mmol, 10 %), which eluted shortly before the α-anomer (yield not determined). ^{1}H NMR (400 MHz, $CDCl_3$): δ = 1.11 (d, J = 7.3 Hz, 18H), 1.29 (sept, J = 7.3 Hz, 3H), 1.37 (d, J = 13.3 Hz, 1H), 2.10–2.25 (m, 2H), 2.39 (s, 3H), 2.42 (s, 3H), 2.49 (dd, J = 13.8, 5.0 Hz, 1H), 3.89–3.96 (m, 2H), 4.15–4.20 (m, 2H), 4.47–4.50 (m, 1H), 4.62 (m, 2H), 5.22 (dd, J = 11.0, 4.9 Hz, 1H), 5.57 (d, J = 5.6 Hz, 1H), 5.84 (s, 1H), 6.73 (d, J = 8.4 Hz, 1H), 7.20–7.29 (m, 5H), 7.58 (d, J = 2.3 Hz, 1H), 7.94–7.97 ppm (m, 4H); ^{13}C NMR (100 MHz, $CDCl_3$): δ = 13.0, 18.0, 21.7, 25.9,

41.7, 65.0, 67.5, 77.4, 80.7, 82.8, 97.4, 118.4, 125.2, 127.0, 128.6, 129.1, 129.2, 129.7, 129.8, 132.8, 143.6, 144.0, 152.8, 166.1, 166.5 ppm; IR (KBr): $\tilde{\nu}$ = 2947 (m), 2867 (m), 1720 (s), 1613 (m), 1500 (m), 1466 (w), 1377 (w), 1275 (s), 1178 (m), 1150 (w), 1098 (s), 1001 (m), 906 (m), 884 cm^{-1} (w); ESI-HRMS: *m/z* calcd for $C_{40}H_{53}O_8Si$ $[M+H]^+$: 689.3510; found: 689.3498.

Deprotected nucleoside 6a: The β-anomer of **6** (303 mg, 0.44 mmol) was dissolved in dry methanol (7 mL) and K_2CO_3 (134 mg, 0.97 mmol) was added. The suspension was stirred for 2 h at room temperature until all the solids had dissolved. The yellow solution was diluted with chloroform (50 mL) and water (50 mL). The aqueous phase was separated and extracted three times with chloroform (50 mL). The combined organic extracts were washed with saturated, aqueous NaCl and dried with Na_2SO_4. After removal of the solvents in vacuo, the raw material was purified by using flash column chromatography (silica gel; $CHCl_3/CH_3OH$ = 10:1) to yield a colorless oil (86 mg, 0.19 mmol, 43 %). ^{1}H NMR (400 MHz, $CDCl_3$): δ = 1.11 (d, *J* = 7.3 Hz, 18H), 1.29 (sept, *J* = 7.3 Hz, 3H), 1.41 (d, *J* = 13.5 Hz, 1H), 1.95–2.04 (m, 1H), 2.13 (dd, *J* = 10.2, 5.6 Hz, 1H), 2.17–2.28 (m, 1H), 2.80 (s, 2 OH), 3.63–3.73 (m, 2H), 3.88–3.97 (m, 3H), 4.20–4.24 (m, 2H), 4.27–4.30 (m, 1H), 5.07 (dd, *J* = 10.2, 5.6 Hz, 1H), 5.86 (s, 1H), 6.75 (d, *J* = 8.4 Hz, 1H), 7.16 (dd, *J* = 8.4, 2.4 Hz, 1H), 7.54 ppm (d, *J* = 2.4 Hz, 1H); ^{13}C NMR (100 MHz, $CDCl_3$): δ = 13.0, 18.0, 25.8, 43.6, 63.3, 67.6, 73.6, 79.9, 87.20, 97.4, 118.2, 125.2, 127.7, 128.5, 133.4, 152.8 ppm; IR (KBr): $\tilde{\nu}$ = 2946 (m), 2868 (m), 1654 (m), 1618 (m), 1500 (m), 1466 (w), 1389 (w), 1279 (m), 1150 (w), 1127 (w), 1095 (m), 1051 (w), 1000 cm^{-1} (w); ESI-HRMS: *m/z* calcd for $C_{24}H_{40}ClO_6Si$ $[M+Cl]^-$: 487.2283; found: 487.2257.

DMT-protected nucleoside 6b: Compound **6a** (86 mg, 0.19 mmol) was coevaporated twice with 2 mL of dry pyridine. It was then dissolved in 1 mL of pyridine and stirred over 4 Å molecular sieves for 2 h. 4,4′-Dimethoxytrityl chloride (71 mg, 0.21 mmol) was then added and the reaction was stirred for 2 h at room temperature. Subsequently, dry methanol (2 mL) was added, the mixture stirred for 1 h, filtered, and the solvents removed in vacuo. Flash chromatography (silica gel; hexane/EtOAc (9:1) + 0.1 % pyridine) yielded a colorless oil (79 mg, 0.11 mmol, 55 %). ^{1}H NMR (400 MHz, $CDCl_3$): δ = 1.11 (d, *J* = 7.6 Hz, 18H), 1.29–1.33 (m, 4H), 2.02–2.11 (m, 2H), 2.17 (dd, *J* = 13.1, 5.6 Hz, 1H), 3.25–3.34 (m, 2H), 3.78 (s, 6H), 3.87–3.93 (m, 2H), 4.01 (m, 1H), 4.09–4.18 (m, 2H), 4.38 (m, 1H), 5.10 (dd, *J* = 10.1, 5.6 Hz, 1H), 5.85 (s, 1H), 6.73 (d, *J* = 8.4 Hz, 1H), 6.82 (d, *J* = 9.0 Hz, 4H), 7.17–7.30 (m, 4H), 7.36 (d, *J* = 9.0 Hz, 4H), 7.48 (d, *J* = 8.3 Hz, 2H), 7.60 ppm (d, *J* = 2.1 Hz, 1H); ^{13}C NMR (150 MHz, $CDCl_3$): δ = 13.0, 18.0, 25.8, 43.9, 55.2, 64.6, 67.4, 74.8, 79.8, 86.1, 97.4, 113.1, 118.1, 125.3, 126.7, 127.3, 127.8, 128.3, 128.6, 130.1, 134.0, 136.2, 144.9, 152.5, 158.4 ppm; IR (KBr): $\tilde{\nu}$ = 1719 (m), 1654 (m), 1618 (m), 1560 (w), 1542 (w), 1508 (m), 1458 (w), 1272 (m), 1097 cm^{-1} (m); ESI-HRMS: *m/z* calcd for $C_{45}H_{59}O_8Si$ $[M+H]^+$: 755.3979; found: 755.3961.

Phosphoramidite 7: Compound **6b** (66 mg, 87 μmol) was coevaporated twice with 2 mL of dry THF and finally dissolved in 2 mL of degassed THF. $NEt(iPr)_2$ (31 μL, 170 μmol) and $(iPr_2N)(NCCH_2CH_2O)PCl$ (28 μL, 130 μmol) were then added and the reaction mixture was stirred for 2 h. The solvents were removed in vacuo and the residue was dissolved in degassed EtOAc (1 mL) and purified by using column chromatography under a protecting gas atmosphere (deactivated silica gel; hexane/EtOAc (2:1) + 0.1 % pyridine; all solvents degassed). The solvent was removed under high vacuum to yield a mixture of diastereomers as a colorless oil (76 mg, 80 μmol, 92 %), which was immediately used in DNA synthesis. ^{1}H NMR (200 MHz, $CDCl_3$): δ = 1.05–1.20 (m, 30H), 1.25–1.33 (m, 4H), 1.96–2.12 (m, 2H), 2.23–2.29 (m, 1H), 2.44 (t, *J* = 6.5 Hz, 2H), 2.61 (t, *J* = 6.5 Hz, 2H), 3.21–3.32 (m, 2H), 3.46–3.74 (m, 2H), 3.77 (s, 3H), 3.78 (s, 3H), 3.90–3.97 (m, 2H), 4.11–4.24 (m, 3H), 4.43–4.45 (m, 1H), 5.10 (dd, *J* = 10.6, 5.0 Hz, 1H), 5.86 (s, 1H), 6.73–6.84 (m, 5H), 7.23–7.31 (m, 4H), 7.35–7.41 (m, 4H), 7.48–7.52 (m, 2H), 7.64 ppm (d, *J* = 2.3 Hz, 1H); ^{31}P NMR (80 MHz, $CDCl_3$): δ = 149.0, 148.6 ppm; ESI-HRMS: *m/z* calcd for $C_{54}H_{76}N_2O_9PSi$ $[M+H]^+$: 955.5058; found: 955.5083.

Deprotected ligand nucleoside 2: β-1′-(4-[1,3]Dioxan-2-yl-3-(triisopropylsilyloxy)phenyl)-2′-desoxyribose (85 mg, 0.17 mmol) was dissolved in dry THF (2 mL), tetrabutylammonium fluoride (1.7 equiv, 1.1 M in THF) was added, and the mixture stirred for 3 h at room temperature. Then, concentrated HCl (200 μL) and one drop of water were added and the mixture stirred for another 2 h. A further 10 mL of water was added and the mixture was extracted three times with Et_2O (20 mL). The combined organic extracts were dried with Na_2SO_4, the solvents removed in vacuo, and the raw product purified by using flash column chromatography (silica gel; $CHCl_3/CH_3OH$ = 9:1). The resulting brown solid was purified by recrystallization from EtOAc to yield colorless needles (15 mg, 0.06 mmol, 32 %). ^{1}H NMR (400 MHz, CD_3OD): δ = 1.90 (ddd, *J* = 13.1, 10.4, 5.9 Hz, 1H), 2.26 (ddd, *J* = 13.1, 10.4, 5.9 Hz, 1H), 3.68 (pseudosept, *J* = 5.1, 11.6 Hz, 2H), 3.98 (dt, *J* = 5.1, 2.4 Hz, 1H), 4.32 (dt, *J* = 5.9, 1.9 Hz, 1H), 5.13 (dd, *J* = 10.4, 5.6 Hz, 1H), 7.03 (s, 1H), 7.06 (dd, *J* = 8.0, 1.4 Hz, 1H), 7.66 (d, *J* = 8.0 Hz, 1H), 9.98 ppm (s, 1H); ^{13}C NMR (100 MHz, CD_3OD): δ = 44.81, 64.01, 74.28, 80.85, 89.50, 115.13, 118.50, 121.87, 134.11, 153.82, 162.79, 196.86 ppm; IR (diamond-ATR): $\tilde{\nu}$ = 3262 (m), 2897 (m), 1650 (s), 1628 (s), 1434 (m), 1348 (m), 1309 (s), 1177 (m), 1153 (s), 1087 (s), 1051 (s), 988 (s), 956 (m), 874 (m), 810 (s), 680 cm^{-1} (m); ESI-HRMS: *m/z* calcd for $C_{12}H_{13}O_5$ $[M-H]^-$: 237.0757; found: 237.0771.

Salen ligand 2b: The fully deprotected ligand **2** (45 mg, 0.19 mmol) was dissolved in dry methanol (10 mL) and ethylenediamine (0.5 equiv, 6.32 μL, 0.095 mmol) was added. The color of the solution changed to yellow and a microcrystalline yellow material precipitated over several days. The reaction was also carried out in CD_3OD in an NMR tube and quantitative conversion was observed by NMR spectroscopy. ^{1}H NMR (400 MHz, CD_3OD): δ = 1.90 (ddd, *J* = 13.2, 10.4, 5.9 Hz, 1H), 2.21 (dtd, *J* = 12.5, 5.2, 1.7 Hz, 1H), 3.53–3.76 (m, 3H), 3.95 (s, 2H), 4.30 (m, 1H), 5.07 (dd, *J* = 10.4, 5.6 Hz, 1H), 6.83–6.93 (m, 2H), 7.30 (dd, *J* = 19.2, 8.0 Hz, 1H), 8.43 ppm (s, 1H); ^{13}C NMR (100 MHz, CD_3OD): δ = 44.85, 59.59, 63.83, 73.95, 80.63, 88.71, 114.38, 115.96, 117.88, 131.75, 147.55, 162.14, 166.12 ppm; IR (diamond-ATR): $\tilde{\nu}$ = 3253 (w), 2890 (w), 2853 (w), 2428 (s), 1984 (w), 1627 (s), 1429 (m), 1372 (m), 1265 (m), 1186 (w), 1138 (m), 1089 (m), 1055 (s), 1021 (s), 976 (s), 938 (m), 898 (m), 866 (m), 816 (s), 808 (s), 755 cm^{-1} (m); ESI-HRMS: *m/z* calcd for $C_{26}H_{33}O_8N_2$ $[M+H]^+$: 501.2231; found: 501.2229.

Cu–salen complex 8: A solution of ligand **2b** (50 mg, 0.10 mmol) in dry methanol (5 mL) was combined with a methanolic solution of $[Cu(acac)_2]$ (26 mg, 0.10 mmol) and heated under reflux for 10 min. The color changed from yellow to green to purple. Slow cooling of a saturated methanolic solution yielded small, dichroic green-purple crystals which were used for crystallographic examination. IR (diamond-ATR): $\tilde{\nu}$ = 3305 (m), 2919 (w), 2888 (w), 1634 (s), 1614 (s), 1526 (s), 1482 (m), 1427 (s), 1387 (m), 1322 (s), 1302 (m), 1312 (m), 1187 (m), 1064 (s), 1038 (s), 998 (s), 966 (s), 959 (s), 873 (s), 795 cm^{-1} (s); ESI-HRMS: *m/z* calcd for $C_{26}H_{31}CuN_2O_8$ $[M+H]^+$: 562.1371; found: 562.1369. For crystallographic data, see ref. [11].

DNA synthesis, cleavage, and purification: DNA synthesis was performed using Ultramild Bases and reagents (Glen Research) and following standard phosphoramidite protocols. The coupling times and amounts of ligands could be reduced to match the parameters for coupling the natural bases. The trityl values showed good incorporation of the modified nucleoside. After additional treatment with 2 % dichloroacetic acid plus 1 % H_2O in dichloromethane to remove the acetal protecting groups, the controlled-pore-size glass (CPG) solid support was treated with concentrated, aqueous NH_3/EtOH (3:1) for 12 h at room temperature to cleave the strands. The solvents were removed in a SpeedVac concentrator and the pellet redissolved in doubly distilled water. Analysis and purification was performed on Merck LaChrome HPLC systems using 5μ Silica-C_{18} RP columns and 0.1 M $NHEt_3OAc$ in H_2O/CH_3CN (typically 0–40 % CH_3CN in 40 min) as eluent. Prior to HPLC purification, 20 % HOAc was added and the mixture incubated for 20 min. The purified fractions were concentrated, desalted on Waters Sepac-C_{18} cartridges, and concentrated again. The concentration was estimated by UV spectroscopy following standard procedures, taking into account the molar extinction coefficient for the ligand **2** (ε = 10290 $L\,mol^{-1}\,cm^{-1}$).

Acknowledgments

We thank the Volkswagen Foundation (Priority program: Complex Materials), the DFG (SFB 486), and the Fonds der chemischen Industrie for a Kekulé Fellowship to G.H.C.

[1] J. D. Watson, F. H. C. Crick, *Nature* **1953**, *171*, 737.
[2] a) L. Orgel, *Science* **2000**, *290*, 1306; b) A. Eschenmoser, R. Krishnamurthy, S. Guntha, P. Scholz, K.-U. Schöning, *Science* **2000**, *290*, 1347.
[3] R. Micura, R. Kudick, S. Pitsch, A. Eschenmoser, *Angew. Chem.* **1999**, *111*, 715; *Angew. Chem. Int. Ed.* **1999**, *38*, 680.
[4] a) N. J. Leonard, *Acc. Chem. Res.* **1982**, *15*, 128; b) H. Liu, J. Gao, S. R. Lynch, Y. D. Saito, L. Maynard, E. T. Kool, *Science* **2003**, *302*, 868.
[5] a) C. Brotschi, C. J. Leumann, *Nucleosides, Nucleotides Nucleic Acids* **2003**, *22*, 1195; b) L. Zhang, E. Meggers, *J. Am. Chem. Soc.* **2005**, *127*, 74; c) N. Zimmerman, E. Meggers, P. G. Schultz, *J. Am. Chem. Soc.* **2002**, *124*, 13684; d) E. Meggers, P. L. Holland, W. B. Tolman, F. E. Romesberg, P. G. Schultz, *J. Am. Chem. Soc.* **2000**, *122*, 10714; e) T. Tanaka, A. Tengeiji, T. Kato, N. Toyama, M. Shiro, M. Shionoya, *J. Am. Chem. Soc.* **2002**, *124*, 12494; f) K. Tanaka, Y. Yamada, M. Shionoya, *J. Am. Chem. Soc.* **2002**, *124*, 8802; g) C. Switzer, S. Sinha, P. H. Kim, B. D. Heuberger, *Angew. Chem.* **2005**, *117*, 1553; *Angew. Chem. Int. Ed.* **2005**, *44*, 1529; h) C. Switzer, D. Shin, *Chem. Commun.* **2005**, 1342; i) H. Weizman, Y. Tor, *J. Am. Chem. Soc.* **2001**, *123*, 3375; j) D. Popescu, T. Parolin, C. Achim, *J. Am. Chem. Soc.* **2003**, *125*, 6354; k) Y. Miyake, H. Togashi, M. Tashiro, H. Yamaguchi, S. Oda, M. Kudo, Y. Tanaka, Y. Kondo, R. Sawa, T. Fujimoto, T. Machinami, A. Ono, *J. Am. Chem. Soc.* **2006**, *128*, 2172.
[6] a) S. Klug, M. Famulok, *Mol. Biol. Rep.* **1994**, *20*, 97; b) D. Zha, A. Eipper, M. T. Reetz, *ChemBioChem.* **2003**, *4*, 34; c) G. Roelfes, B. L. Feringa, *Angew. Chem.* **2005**, *117*, 3294; *Angew. Chem. Int. Ed.* **2005**, *44*, 3230.
[7] K. Tanaka, A. Tengeiji, T. Kato, N. Toyama, M. Shionoya, *Science* **2003**, *299*, 1212.
[8] G. H. Clever, K. Polborn, T. Carell, *Angew. Chem.* **2005**, *117*, 7370; *Angew. Chem. Int. Ed.* **2005**, *44*, 7204.
[9] R. X.-F. Ren, N. C. Chaudhuri, P. L. Paris, S. Rumney IV, E. T. Kool, *J. Am. Chem. Soc.* **1996**, *118*, 7671.
[10] G. Zemplén, E. Pascu, *Ber. Dtsch. Chem. Ges.* **1929**, *62*, 1613.
[11] CCDC-602317 contains the supplementary crystallographic data for this paper. These data can be obtained free of charge from The Cambridge Crystallographic Data Centre via www.ccdc.cam.ac.uk/data_request/cif.
[12] a) D. Hall, T. N. Waters, *J. Chem. Soc.* **1960**, 2644; b) L. C. Nathan, J. E. Koehne, J. M. Gilmore, K. A. Hannibal, W. E. Dewhirst, T. D. Mai, *Polyhedron* **2003**, *22*, 887; c) L. Dyers Jr., S. Y. Que, D. VanDerveer, X. R. Bu, *Inorg. Chim. Acta* **2006**, *359*, 197.
[13] W. Saenger, *Principles of Nucleic Acid Structures*, Springer, New York, **1984**, pp. 9–27.
[14] S. Akine, T. Taniguchi, T. Nabeshima, *Chem. Lett.* **2001**, *7*, 682.
[15] a) S. Zolezzi, A. Decinti, E. Spodine, *Polyhedron* **1999**, *18*, 897; b) R. Klement, F. Stock, H. Elias, H. Paulus, P. Pelikán, M. Valko, M. Mazúr, *Polyhedron* **1999**, *18*, 3617.
[16] R. S. Downing, F. L. Urbach, *J. Am. Chem. Soc.* **1969**, *91*, 5977.
[17] a) J. H. Banoub, R. P. Newton, E. Esmans, D. F. Ewing, G. Mackenzie, *Chem. Rev.* **2005**, *105*, 1869; b) S. A. Hofstadler, R. H. Griffey, *Chem. Rev.* **2001**, *101*, 377; c) J. L. Beck, M. L. Colgrave, S. F. Ralph, M. M. Sheil, *Mass Spectrom. Rev.* **2001**, *20*, 61.
[18] J. F. Larrow, E. N. Jacobsen, *J. Org. Chem.* **1994**, *59*, 1939.
[19] M. Hoffer, *Chem. Ber.* **1960**, *93*, 2777.

Received: April 20, 2006
Published online: September 19, 2006

